JACS
JOURNAL OF THE AMERICAN CHEMICAL SOCIETY

Article

pubs.acs.org/JACS

Pre-Gating Conformational Changes in the ChETA Variant of Channelrhodopsin-2 Monitored by Nanosecond IR Spectroscopy

Víctor A. Lórenz-Fonfría,*[,†] Bernd-Joachim Schultz,[†] Tom Resler,[†] Ramona Schlesinger,[‡] Christian Bamann,[§] Ernst Bamberg,[§] and Joachim Heberle[†]

[†]Experimental Molecular Biophysics, Department of Physics, Freie Universität Berlin, Arnimallee 14, 14195 Berlin, Germany
[‡]Genetic Biophysics, Department of Physics, Freie Universität Berlin, Arnimallee 14, 14195 Berlin, Germany
[§]Biophysical Chemistry, Max Planck Institute of Biophysics, Max-von-Laue-Straße 3, 60438 Frankfurt am Main, Germany

Supporting Information

ABSTRACT: Light-gated ion permeation by channelrhodopsin-2 (ChR2) relies on the photoisomerization of the retinal chromophore and the subsequent photocycle, leading to the formation (on-gating) and decay (off-gating) of the conductive state. Here, we have analyzed the photocycle of a fast-cycling ChR2 variant (E123T mutation, also known as ChETA), by time-resolved UV/vis, step-scan FT-IR, and tunable quantum cascade laser IR spectroscopies with nanosecond resolution. Pre-gating conformational changes rise with a half-life of 200 ns, silent to UV/vis but detected by IR spectroscopy. They involve changes in the peptide backbone and in the H-bond of the side chain of the critical residue D156. Thus, the P_1^{500} intermediate must be separated into early and late states. Light-adapted ChR2 contains a mixture of all-*trans* and 13-*cis* retinal in a 70:30 ratio which are both photoactive. Analysis of ethylenic and fingerprint vibrations of retinal provides evidence that the 13-*cis* photocycle recovers in 1 ms. This recovery is faster than channel off-gating and most of the proton transfer reactions, implying that the 13-*cis* photocycle is of minor functional relevance for ChR2.

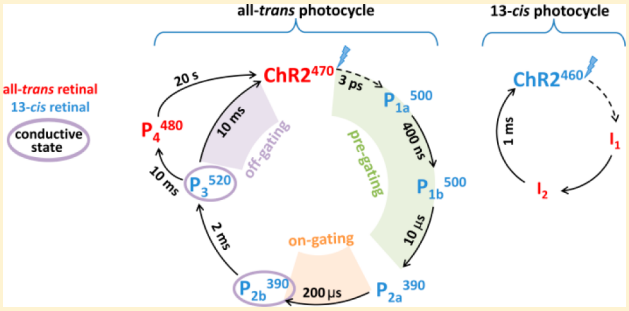

INTRODUCTION

Channelrhodopsins (ChR's) have become renowned for being the only light-gated ion channels known in nature up to now. Light-driven passive conductance for cations by ChR's was proven in ground-breaking electrophysiological experiments on *Xenopus* oocytes and HEK cells expressing ChR1 and ChR2 from the green alga *Chlamydomonas reinhardtii*.[1,2] In subsequent proof-of-principle experiments, the channel activity of ChR2 was shown as sufficient to depolarize the cell membrane when expressed in a host cell, and soon later used as an optogenetic tool to trigger action potential in excitable cells.[3,4] ChR2 and ChR2-based variants remain the most used and best characterized ChR's to date.[5−8]

ChR's belong to the family of microbial (type-I) rhodopsins, characterized by a seven-transmembrane helical fold of the apoprotein (opsin) and the presence of a retinal chromophore covalently linked to a lysine to form a protonated Schiff base (SB).[9,10] The light-gated channel activity of ChR's, and of ChR2 in particular, relies on the photoisomerization of the retinal chromophore around the $C_{13}{=}C_{14}$ bond. Retinal isomerization is followed by a series of thermal reactions extending from the retinal to the apoprotein, eventually leading to the start ($t_{1/2}$ ~200 μs) and later to the end ($t_{1/2}$ ~10 ms) of cation permeation, also referred to as channel on- and off-gating, respectively.[5,7] Finally, the initial dark state recovers with $t_{1/2}$ ~20 s at room temperature.[5,7] This cyclic reaction, known as the photocycle, comprises the dark-state $ChR2^{470}$ and at least four intermediate states known as P_1^{500}, P_2^{390}, P_3^{520}, and P_4^{480}, where the superscript indicates the absorption maximum of the retinal in the wild-type (WT) form.[5,7] According to various pieces of evidence, only a late P_2^{390} and the P_3^{520} intermediate are cation-conductive states.[7]

The crystal structure of the dark state of a chimera constructed from ChR1 and ChR2 of *C. reinhardtii* (C1C2) was determined to a resolution of 2.3 Å,[11] providing a structural framework to address the molecular mechanism of the channel activity of ChR's. Although the structural model corresponds to the closed state of the channel, helices A, B, C, and G form a vestibule where cations could diffuse half way across the membranous part of the protein.[11] Recent results from interhelical distances inferred by pELDOR spectroscopy on a ChR2-C128T-like variant suggested that helices B and F move in the P_3^{520} intermediate, presumably opening the vestibule framed by helices A, B, C, and G in the dark state to form a continuous pore.[12] These helical movements partially persist in the P_4^{480} intermediate.[13]

Received: October 22, 2014
Published: January 13, 2015

DOI: 10.1021/ja5108595
J. Am. Chem. Soc. 2015, 137, 1850−1861

IR spectroscopic studies pointed to substantial conformational changes preceding the onset of the photocurrents[14−16] to which we refer to as pre-gating conformational changes. Although insufficient to lead to cation permeation, they presumably form part of the chain of molecular events leading to the opening of the channel and to the start of cation permeation at a later stage. However, these studies have been mostly limited to steady-state FT-IR experiments at liquid nitrogen temperature.[14,15] More recently, an ultrafast Vis-pump/IR-probe study[17] and a time-resolved step-scan FT-IR study,[16] covering the picosecond and microsecond range, respectively, have also reported pre-gating structural changes. During the review of the present manuscript, a nanosecond step-scan FT-IR experiment on ChR2 was presented.[18] However, the conformational changes taking place in the nanoseconds and early microseconds remain largely unexplored by structurally sensitive methods.

The dark states of ChR1 and ChR2 contain a mixture of all-*trans*,15-*anti* and 13-*cis*,15-*syn* retinal in a 70:30 ratio.[19,20] Although often ignored, each retinal isomer may potentially lead to a photocycle running in parallel after excitation. While the all-*trans* photocycle of ChR2 is evidently functional, i.e., leads to the formation of a conductive state, experimental evidence regarding the functionality of the 13-*cis* photocycle is inconclusive.[7] Quantitative modeling of the photocurrents of ChR1 and ChR2 recorded under continuous illumination indicates the presence of two parallel photocycles,[21,22] each with a conductive state differing in cation conductivity/selectivity,[23] as well as in off-gating kinetics.[22] Recently, it was suggested that the all-*trans* and 13-*cis* retinal isomers present in the dark state of ChR2 might account for these two parallel photocycles.[24]

Here, we characterized the photocycle of the ChR2-E123T variant by flash-photolysis UV/vis spectroscopy, step-scan FT-IR spectroscopy, and tunable quantum cascade laser (QCL) IR spectroscopy, all with nanosecond time resolution. ChR2 with the E123T mutation (also known as ChETA in optogentic applications) was introduced as an ultrafast channelrhodopsin.[25] It shows twice faster channel off-gating (τ = 5 ms vs 9 ms) and 10-fold faster dark-state recovery (τ = 1 s vs 11 s) than wild-type ChR2 (ChR2-WT) according to electrophysiological experiments.[25] Femtosecond pump−probe UV/vis experiments revealed that retinal photoisomerization steps are at most 2-fold delayed in ChR2-E123T with respect to the WT form.[26] We confirm here that the E123T exchange has an effect on the electrostatic environment of the retinal but a reduced effect in the kinetics of the photocycle, with the exception of the 5-fold accelerated dark-state recovery from P_4^{480}. Taking advantage of its faster but still native-like photocycle, we obtained new information on pre-gating conformational changes taking place on the nanosecond scale. Furthermore, analysis of C═C and C—C stretching vibrations of the retinal, notably sensitive to the retinal conformation, unraveled molecular signatures of the all-*trans* and 13-*cis* photocycles. We extrapolate these results to the photocycle of ChR2-WT.

RESULTS AND DISCUSSION

The E123T Mutation Affects the Electrostatic Environment of the Retinal. Light absorption in the UV/vis region originates from the retinal chromophore, with the maximum wavelength λ_{max} critically sensitive to the protonation state of the Schiff base (SB) and the conformation of its polyene chain. Furthermore, λ_{max} is sensitive to the local electrostatic environment around the retinal because the electronic ground and excited states differ in their charge distribution when the SB is protonated.[27,28]

The absorption spectrum of retinal in ChR2-WT exhibits a characteristic fine structure,[14] best resolved in the second derivative spectrum (blue traces in Figure 1). The fine

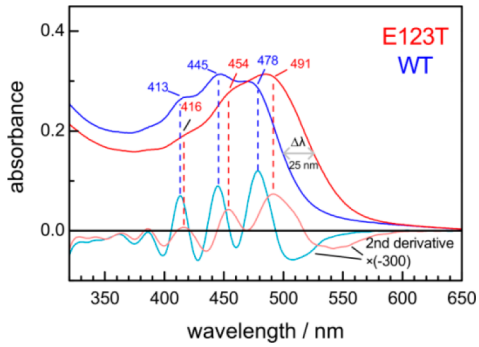

Figure 1. UV/vis spectra of wild-type ChR2 (WT, blue lines) and the E123T variant (red lines) solubilized in 0.1% DM (100 mM NaCl, 20 mM Hepes, pH 7.4) and their (minus) second derivatives (faint colors).

structure, not commonly resolved in retinal proteins but clearly resolved in sensory rhodopsin II,[29] has been assigned to the coupling between the electronic $S_0 \rightarrow S_1$ transition with vibrational transitions $\nu = 0 \rightarrow \nu' = (0, 1, ...)$, with peaks at 478.5 nm ($\nu = 0 \rightarrow \nu' = 0$), 445 nm ($\nu = 0 \rightarrow \nu' = 1$), and 413 nm ($\nu = 0 \rightarrow \nu' = 2$).[7] In ChR2-E123T, the absorption spectrum of retinal (red spectrum in Figure 1), as well as the action spectrum for channel conductance,[25] appears red-shifted by ∼25−20 nm with respect to ChR2-WT. The fine structure is broader but still resolved in the second derivative spectrum, with maxima at 491.5, 453.5, and 416 nm. Consequently, the pure electronic transition ($\nu = 0 \rightarrow \nu' = 0$) upon E123T exchange is in fact shifted by ∼13 nm. The relative destabilization of the electronic ground state in ChR2-E123T by ∼0.07 eV is compatible with neutralization of an acidic residue near the retinal SB; i.e., it sustains an anionic E123 side chain in wild-type ChR2, in accordance with empirical and QM/MM calculations.[11,30] In comparison, neutralization of D85 in bR (the homogeneous residue to E123) by acidic pH or site-directed mutagenesis leads to a red-shift from 568 to ∼600 nm (∼0.12 eV).[31]

ChR2-E123T Shows a WT-like Photocycle. The photocycle of the E123T mutant of ChR2 was recorded by time-resolved UV/vis spectroscopy. Figure 2a provides a color-coded surface representation of the transient absorption changes following a 10 ns pulsed laser excitation. The spectro-temporal changes of the photocycle of ChR2-E123T are qualitatively similar to those of ChR2-WT (Figure 2b). Both variants show an early red-shifted intermediate (P_1^{500}, t_{max} < 100 ns), a blue-shifted intermediate (P_2^{390}, t_{max} = 150 μs in ChR2-WT and 250 μs in ChR2-E123T), a late red-shifted intermediate (P_3^{520}, t_{max} = 3 ms in ChR2-WT and 4 ms in ChR2-E123T), and a slowly decaying dark-state-like intermediate (P_4^{480}, $t_{max} \approx$ 200−300 ms). Note that the nomenclature of ChR2-WT is used for intermediates of the ChR2-E123T photocycle, despite differences in their λ_{max}. The main kinetic alteration in the photocycle of ChR2-E123T is the ∼4 times faster recovery of the dark state from P_4^{480} compared to ChR2-WT: τ = 3 s in

DOI: 10.1021/ja5108595
J. Am. Chem. Soc. 2015, 137, 1850−1861

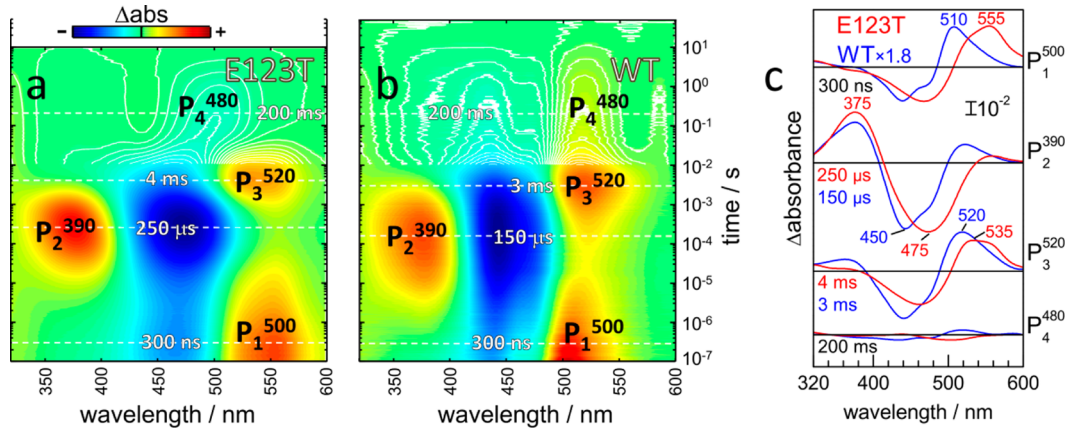

Figure 2. Light-induced absorption difference maps of (a) ChR2-E123T and (b) ChR2-WT in the UV/vis range. Contour lines after 10 ms are provided for a better appreciation of the decay kinetics. Dashed horizontal lines indicate spectral slices shown in part c. (c) Absorption difference spectra of ChR2-E123T (red lines) and ChR2-WT (blue lines) at times where specific intermediates maximally accumulate.

ChR2-E123T (see Table S1, Supporting Information) vs τ = 12 s in ChR2-WT for the slower time constant.[16]

The parent state and the intermediates P_1^{500} and P_3^{520} are red-shifted in ChR2-E123T with respect to ChR2-WT by approximately 25, 45, and 15 nm, respectively (Figure 2c). The observed shifts are compatible with the neutralization of an acidic residue near the retinal SB upon the E123T mutation in these three states. The λ_{max} of the P_2^{390} intermediate appears insensitive to the E123T mutation (Figure 2c), as otherwise expected for an intermediate with unprotonated (neutral) SB and, thus, largely insensitive to electrostatic changes in the proximity of the retinal.[10] Overall, the spectral shifts indicate that E123 remains ionic throughout the photocycle of ChR2-WT.[16]

Nanosecond Time-Resolved Infrared Difference Spectroscopy on ChR2-E123T. To elucidate the early dynamics of the opsin and the retinal, as well as to unravel contributions from the all-*trans* and 13-*cis* photocycle, we performed time-resolved IR experiments. Time-resolved step-scan FT-IR experiments on hydrated films of ChR2-E123T were recorded at an instrumental temporal resolution of 60 ns (see Figure 3 and the Experimental Section), which is 2 orders of magnitude improved with respect to our previous experiments on ChR2-WT.[16] Figure 3b (gray) shows spectral slices taken at 300 ns, 300 μs, 4 ms, and 200 ms after the exciting laser pulse corresponding to vibrational changes of the P_1^{500}, P_2^{390}, P_3^{520}, and P_4^{480} intermediate states of ChR2-E123T (see Figure 2 in Lórenz-Fonfría et al.[16] for FT-IR difference spectra of ChR2-WT).

To resolve early changes in the amide I (1610−1680 cm^{-1}) and carboxylic (1700−1780 cm^{-1}) regions, complementary experiments applying a tunable quantum cascade laser (QCL) as the IR light source (Figure 3b, black spectra) were performed with a time resolution of 15 ns (see the Experimental Section). Experiments reassured that the protein films were sufficiently hydrated, as the t_{max} of the intermediates was only marginally delayed in hydrated films with respect to ChR2 dissolved in solution: 250 μs vs 300 μs for P_2^{390} and 4 ms vs 5 ms for P_3^{520} (Figure S1, Supporting Information). Accordingly, the time constants provided by global exponential fitting are almost identical for ChR2-E123T in solution and in hydrated films (Table S1, Supporting Information).

Pre-Gating Conformational Changes in the Opsin Moiety Indicate the Presence of Two P_1^{500} Substates.

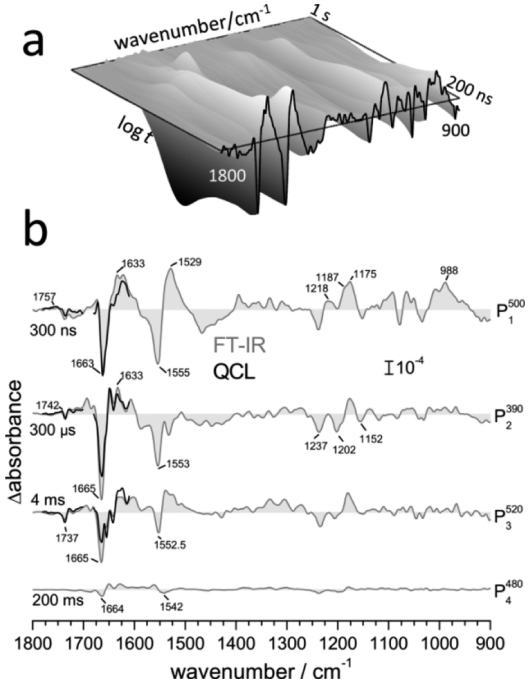

Figure 3. Time-resolved IR difference spectra of ChR2-E123T. (a) 3D plot of the time-resolved FT-IR data after global exponential fitting. (b) Experimental FT-IR (gray) and QCL (black) difference spectra at selected times where specific intermediates maximally accumulate according to UV/vis experiments displayed in Figure 2. QCL spectra were scaled by 0.25 to fit the FT-IR spectra. Differences between FT-IR and QCL spectra can be accounted for by their different spectral resolutions of 8 and 4 cm^{-1}, respectively.

Early spectral changes in the amide I region in ChR2-E123T are dominated by an intense negative band at ∼1663 cm^{-1} (see Figure 3). Light-induced FT-IR difference spectra of ChR2-WT at 80 K resolved a similarly intense negative band at ∼1664 cm^{-1}.[14,15] We noted before for ChR2-WT that the transient absorption changes of a positive band at 1633 cm^{-1} mirror those from the negative band at 1662 cm^{-1}.[16] From this observation, we tentatively assigned them to the elongation of β-strands (positive band at 1633 cm^{-1}) from loops (negative band at 1662 cm^{-1}),[16] both present in the extra-membrane parts of the C1C2 chimera.[11] However, the superior time resolution of our current QCL experiments shows that the

DOI: 10.1021/ja5108595
J. Am. Chem. Soc. 2015, 137, 1850−1861

negative absorption changes at 1662 cm^{-1} rise in less than 15 ns, the response time of the detection system (Figure 4a,

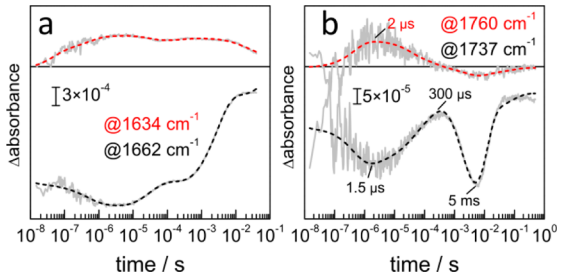

Figure 4. Experimental (continuous gray) and globally fitted (dashed red/black traces) transient QCL absorption changes of ChR2-E123T: (a) at 1662 and 1634 cm^{-1}; (b) at 1760 and 1737 cm^{-1}.

black), while at 1634 cm^{-1} they rise with $t_{1/2} \approx 200$ ns (Figure 4a, red). Therefore, the negative band at 1663 cm^{-1} rises almost instantaneously, and lacks any clear positive counterpart of equivalent intensity (Figure 3b).

As will be shown below (Figure 5a), the band at 1663 cm^{-1} is largely devoid of contributions from the C=N stretch of the

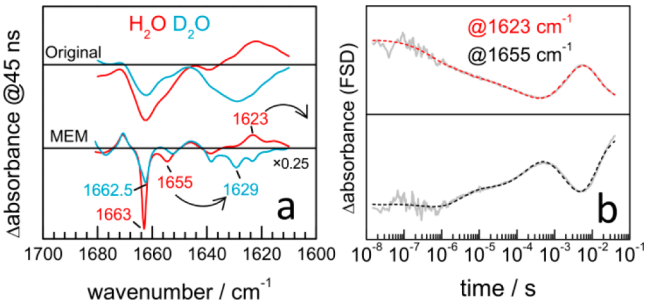

Figure 5. (a) IR difference spectra of ChR2-E123T for samples rehydrated with H_2O (red lines) and D_2O (blue lines). (top) Spectra 45 ns after photoexcitation recorded by QCL experiments, processed to 4 cm^{-1} resolution. (bottom) Spectra after application of band-narrowing by MEM. The arrows indicate shifts of bands assigned to the C=N vibration of the SB upon deuteration. (b) Transient absorption changes at 1655 and 1623 cm^{-1} (gray traces) and after global exponential fitting (dashed red/black traces).

SB and resistant to H/D exchange and, thus, most likely originates from an amide I vibration, a mode mostly contributed by the C=O stretching vibration of the amide group of the protein backbone. In proteins, amide I vibrations are strongly coupled,[32] and are generally resistant to H/D exchange when localized in transmembrane regions.[33] Thus, the negative band at 1663 cm^{-1} might report an ultrafast bend/deformation of a transmembrane helix in contact with the retinal, a distortion expected to reduce the coupling/delocalization (and extinction coefficient) of the amide I vibration of an helix.[34] The transient absorption changes at 1662 cm^{-1} shows an additional negative rise with $t_{1/2} \approx 200$ ns (Figure 4a), which correlates with the rise of the band at 1633 cm^{-1}.

Regardless of the specific assignment of the spectral changes in the amide I region, the above observations indicate that ultrafast spectral changes occur almost instantaneously after photoexcitation, as previously concluded from fs IR experiments.[17] Additional slower changes occur with $t_{1/2} \approx 200$ ns, reported here for the first time. Because P_1^{500} is the only intermediate present at 200 ns according to UV/vis experiments (see Figure 2), we infer the presence of at least two P_1^{500} substates. The half-life for their transition is 200 ns in ChR2-E123T.

Many spectroscopic and electrophysiology experiments have addressed the critical role of D156 during the photocycle of ChR2,[7] and its functional importance for off-gating kinetics.[16,35] D156 was, moreover, identified as the proton donor of the SB.[16] A negative band at 1737 cm^{-1} (see Figure 3b) has been assigned to the C=O vibration of the side chain of aspartic acid 156.[36] Figure 4b (black) shows the transient absorption changes at 1737 cm^{-1} in the ChR2-E123T variant recorded by the time-resolved tunable QCL setup (see Figure S2, Supporting Information, for equivalent transients recorded by step-scan FT-IR spectroscopy). The initial negative intensity rises in two steps: half of it rises before the response time of the detector (<15 ns), and the remaining half does it with $t_{1/2} \approx$ 200 ns. The negative absorption changes at 1737 cm^{-1} in this time scale can be assigned to the shift of the carboxylic C=O frequency,[16] presumably caused by changes in H-bonding to the terminal S—H of C128.[36] Indeed, it was reported in cryogenic experiments on ChR2-WT that the C=O stretch of D156 shifts from 1737 to 1742 cm^{-1} upon formation of P_1^{500},[15,36] later shown to correspond to a transient state probed at 100 ps after photoexcitation by Vis-pump/IR-probe spectroscopy at room temperature.[17] Thus, the unresolved ultrafast negative rise at 1737 cm^{-1} can be safely assigned to the formation of an early P_1^{500} intermediate.

Previous time-resolved FT-IR experiments on ChR2-WT indicated that the C=O frequency of D156 shifts to a broad band at 1760 cm^{-1} in the early microseconds.[16] However, the time at which this shift occurs could not be determined due to insufficient time resolution. Recently, the band at 1760 cm^{-1} was assigned instead to the C=O stretch of E123.[18] However, a broad positive band at ~1760 cm^{-1} is still observed in the early microseconds of ChR2-E123T (Figure S10, Supporting Information). Albeit showing half the intensity as that in ChR2-WT, the persistence of this band in the E123T variant is at odds with its assignment to E123. Due to the superior time resolution of the current experiments, we were able to determine the rise of the absorption changes at 1760 cm^{-1} to be $t_{1/2} \approx 200$ ns (Figure 4b). The kinetics at 1760 cm^{-1} matches very well with the rise of the negative band at 1737 cm^{-1} from D156 (Figure 4b), supporting the assignment of the former positive band to D156. In addition, this observation gives further support to the presence of two P_1^{500} substates, which therefore not only differ in the peptide backbone conformation but also in the strength of the interhelical H-bond between D156 (helix D) and C128 (helix C). We infer furthermore that the late P_1^{500} intermediate accumulates maximally at around 2 μs in ChR2-E123T (Figure 4b).

Incidentally, we have previously shown that the C=O stretch of D156 shifts from 1760 to 1745 cm^{-1} in the P_2^{390} intermediate of ChR2-WT.[16] For ChR2-E123T, this process is reflected by the appearance of a positive band at 1742 cm^{-1} in P_2^{390} (Figure 3b) and by the decrease of the absorption changes at 1737 cm^{-1} to return at 300 μs to the levels present in the early P_1^{500} intermediate (Figure 4b). Additionally, the transient absorption changes at 1737 cm^{-1} become maximally negative in the P_3^{520} intermediate, at 5 ms, as the SB reprotonates from D156. These observations agree well with those reported before for ChR2-WT.[16]

DOI: 10.1021/ja5108595
J. Am. Chem. Soc. 2015, 137, 1850−1861

The Hydrogen Bonding Strength of the Retinal Schiff Base C═N Weakens after Photoisomerization. The strong negative band at 1663 cm^{-1} shows a shoulder in the nanosecond range, resolved at 1655 cm^{-1} after band-narrowing by deconvolution using the maximum entropy method (MEM, Figure 5a). MEM is a nonlinear reconstruction method,[37] powerful and robust at resolving strongly overlapping components in difference spectra.[38] The position of the band at 1655 cm^{-1} matches well the frequency of the C═N stretching vibration of the SB in the dark state of all-*trans* retinal in ChR2-WT, as resolved by resonance Raman spectroscopy at 1657 cm^{-1}.[19] To further support this assignment, we performed equivalent time-resolved QCL experiments in D_2O. The band at 1655 cm^{-1} shifted to 1629 cm^{-1}, as evident after MEM deconvolution (Figure 5a). The new band corresponds excellently well with the SB C═N stretching at 1629 cm^{-1} resolved by resonance Raman experiments in D_2O.[19] The current assignment convincingly shows that the intense negative band at 1663 cm^{-1} does not originate from the retinal SB C═N stretching but predominantly from an amide I vibration. The intensity of the 1663 cm^{-1} band was reduced in D_2O though. This decrease in intensity cannot be accounted for by partial hydrogen/deuterium exchange of the amide N—H group, as this would lead to a frequency downshift of 5−10 cm^{-1} for the amide I vibration.[39]

The positive band at 1623 cm^{-1} (Figure 5a) may correspond to the νC═N frequency of the SB after retinal isomerization. To support this tentative assignment, we compared the transient absorption changes at 1655 and 1623 cm^{-1} (Figure 5b). These two kinetics were monitored after Fourier self-deconvolution (FSD), a linear deconvolution method with modest narrowing capabilities[40] but suitable to follow time traces of selected bands with enhanced selectivity.[41] As can be seen from Figure 5b, both kinetic traces are almost mirror images, favoring a common molecular origin. Both bands rise faster than the detector response time, and display a decay extending until the late microseconds (Figure 5b).

The putative 32 cm^{-1} downshift of the retinal νC═N in ChR2-E123T (from 1655 to 1623 cm^{-1}) is similar in magnitude to the 31 cm^{-1} downshift following retinal isomerization in bR (from 1640 to 1609 cm^{-1}).[42,43] Thus, retinal isomerization weakens the H-bond of the SB in ChR2, as previously concluded for the C1C2 chimera[44] and for other microbial rhodopsins.[10] In contrast, in bovine rhodopsin, the archetypical animal rhodopsin, the H-bond strength of the SB is not altered by retinal photoisomerization.[45,46] The weakening of the H-bond of the SB and of the surrounding water molecules in bR was proposed to store as much as 46 kJ/mol of the energy deposited in the retinal after photoexcitation,[10,47] energy used to drive posterior proton transfer coupled thermal reactions. The similar downshift of the νC═N in ChR2-E123T and bR suggests that the same rationale might apply to ChR2. However, while the low C═N frequency in the K intermediate of bR (1609 cm^{-1}) indicates that the SB loses its H-bond right after photoisomerization, supported also by structural data,[48] the higher frequency in ChR2-E123T (1623 cm^{-1}) suggests that the SB still remains H-bonded, even if weakly.

Early Intermediates Contain a Twisted Retinal. Hydrogen out-of-plane (HOOP) wagging vibrations of the retinal molecule are Raman as well as IR inactive as long as the retinal polyene chain is planar.[42] Consequently, positive bands assignable to HOOP vibrations in the IR difference spectra are indicative of intermediates with a twisted retinal, or at least more twisted than in the dark state. We tentatively assign the positive band at 988 cm^{-1} in ChR2-E123T (Figure 3) and in ChR2-WT[16] to a HOOP vibration, in analogy to the positive HOOP band at 983 cm^{-1} in bR[42,49,50] and in between 995 and 965 cm^{-1} in early intermediates of several microbial rhodopsins.[51−53] The kinetics of this band in ChR2-E123T (Figure 6) suggests that early intermediates in ChR2 display a twisted retinal. The retinal gradually relaxes to eventually planarize like in the dark state as the photocycle advances. The twist in the retinal is proposed to act as a temporary storage for part of the energy deposited by light in the retinal.[10]

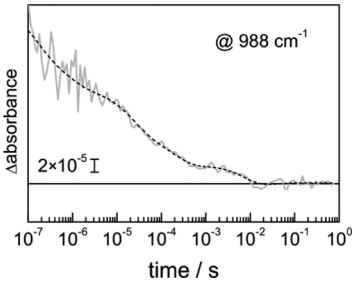

Figure 6. Experimental (gray trace) and fitted (dashed black trace) transient absorption changes of the HOOP band at 988 cm^{-1} extracted from step-scan FT-IR data.

Ethylenic Bands of Retinal Resolve Two Dark States Corresponding to All-*trans* and 13-*cis* Retinal. The polyene chain of retinal contains four C═C bonds whose vibrational modes couple into four ethylenic vibrational modes.[54−56] Most of the IR (and Raman) intensity is concentrated in a single in-phase vibrational mode,[56−58] with the frequency of its oscillation sensitive to the retinal conformation/environment[42,57,58] and correlating with the electronic transition ($1/\lambda_{max}$) in the visible.[59]

Figure 7a depicts time slices of the FT-IR difference spectra. Their comparison with the UV/vis absorption changes at similar times (Figure 7b) is relevant for the discrimination of bands due to ethylenic vibrations of the retinal and those originating from vibrations of the opsin moiety (mostly amide II vibrations). As an example, the intense negative band at ∼1554 cm^{-1} is assigned to the ethylenic vibration of the retinal in the dark state, correlating well with the negative band at ∼470 nm in the UV/vis (see Figure 7a and b). The negative intensity at 1554 cm^{-1} rises within the detector response time (Figure 7c) as expected for an ultrafast retinal photoisomerization.[17,60] The intensity at 1554 cm^{-1} decays to zero in tens of milliseconds. The intensity decrease is a consequence of both dark-state recovery and the formation of P_4^{480}, an intermediate with a dark-state-like λ_{max} (Figure 2c) and, thus, similar ethylenic frequency.

The maximum of the negative band at ∼1554 cm^{-1} shifts during the photocycle (Figure 3) from 1555.5 to 1552 cm^{-1} (Figure 7d), suggesting the spectral overlap of at least two components. In fact, MEM deconvolution resolved the negative band at ∼1554 cm^{-1} into two components (Figure 7a, blue spectra). The most intense with a maximum at ∼1552 cm^{-1} is accompanied by a minor band at ∼1558 cm^{-1}. We assign these two components to the ethylenic vibration of all-*trans*,15-*anti* and 13-*cis*,15-*syn* retinal in the dark state, respectively. This assignment is supported by a previous resonance Raman and retinal extraction study of the dark state of ChR2-WT, revealing

DOI: 10.1021/ja5108595
J. Am. Chem. Soc. 2015, 137, 1850−1861

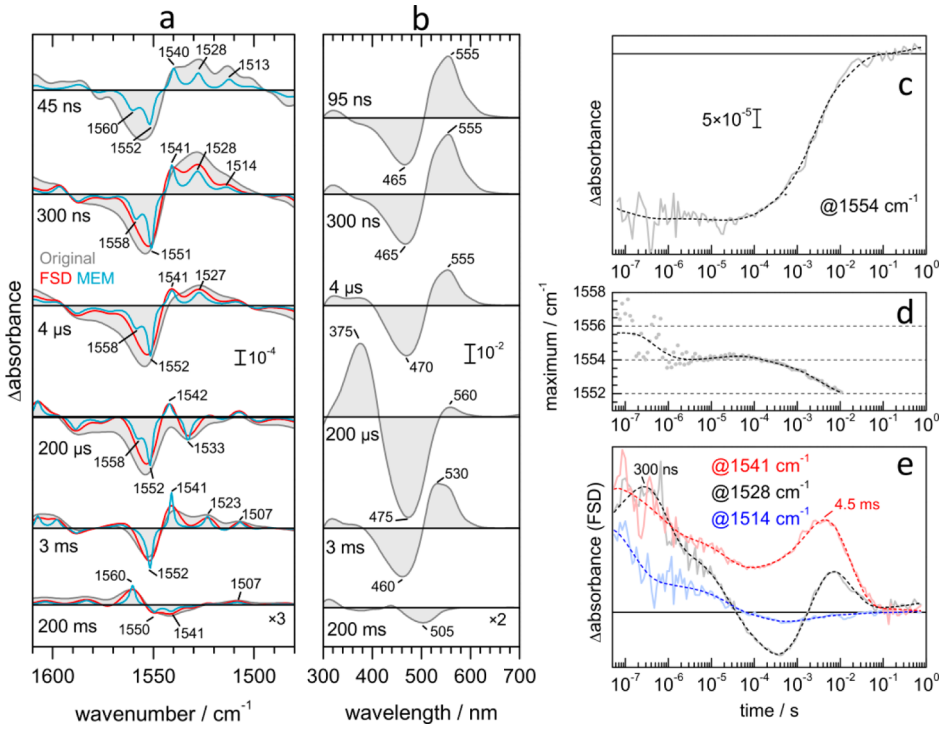

Figure 7. Analysis of the retinal ethylenic region of ChR2-E123T. (a) FT-IR difference spectra of ChR2-E123T at selected times (gray) and processed by two band-narrowing methods: FSD (red) and MEM (light blue). (b) UV/vis difference spectra at equivalent times. Note the different amplification factors at 200 ms in parts a and b. (c) Experimental transient absorption changes of the retinal ethylenic vibration of the dark state at 1554 cm^{-1} (continuous gray trace). (d) Experimental maximum of the retinal ethylenic band of the dark state as a function of time (gray dots). Values above 10 ms are omitted due to the low intensity of the band (see part c). (e) Experimental transient absorption changes at 1541 cm^{-1} (red trace), 1528 cm^{-1} (black trace), and 1514 cm^{-1} (blue trace), monitored by the FSD spectra. In parts c–e, the dashed traces correspond to a global exponential fitting to the experimental data.

a mixture of all-*trans* (70%) and 13-*cis* (30%) retinal isomers, with ethylenic vibrations at 1550 and 1557 cm^{-1}, respectively.[19] Retinal extraction on ChR2-E123T exhibited, similarly to ChR2-WT, a dark state composed of all-*trans* (75%) and 13-*cis* (25%) retinal.[24] Noteworthy, the 1558/1552 cm^{-1} component bands in the difference spectrum of ChR2-E123T represent 30%/70% of the total area of the 1554 cm^{-1} band in the early microseconds. Above 1 ms, only the component at 1552 cm^{-1} was resolved (Figure 7a). We estimate that the component at 1558 cm^{-1} contributes ≤10% to the total area of the ∼1554 cm^{-1} ethylenic band from 1 ms onward. Thus, the photocycle from the 13-*cis* photocycle shows a dark-state recovery with a half-life below 1 ms.

Ethylenic Bands from the Photoproducts of the All-*trans* and 13-*cis* Photocycles. Positive bands assignable to ethylenic vibrations provide information about the products of retinal photoisomerization. We will mainly focus on the characterization of photoproducts preceding the deprotonation of the SB (<10 μs). The early broad positive band at ∼1529 cm^{-1} (Figure 3) shows three components at ∼1540, 1528, and 1514 cm^{-1}, resolved after band narrowing by both FSD and MEM (Figure 7a). From these three putative ethylenic bands, we can infer a λ_{max} value for the retinal absorption in the visible at ∼520, ∼560, and ∼620 nm, respectively,[59] in coherence with the broad positive band centered at 555 nm in the UV/vis difference spectra in the nanosecond range (Figure 7b). Figure 7e shows the transient absorption changes at the wavenumber maxima of these three ethylenic bands, monitored after FSD to reduce cross-contamination in their kinetics. The absorption changes at 1541 and 1514 cm^{-1} rise with the detector response time, i.e., before 60 ns (Figure 7d), while the intensity at 1528 cm^{-1} rises slightly after the detector response time. The positive band at ∼1540 cm^{-1} (λ_{max} ∼520 nm) agrees well with the expected ethylenic band for the P_1^{500} intermediate. The bands at 1528 and 1514 cm^{-1} (λ_{max} ∼560 and ∼620 nm) probably originate from all-*trans* photoproducts of the 13-*cis* photocycle.

The band at 1541 cm^{-1} reaches maximal accumulation at about 4 ms in both ChR2-E123T (Figure 7a,e) and ChR2-WT (Figure S3, Supporting Information). This time is in reasonable agreement with the maximal accumulation of P_3^{520} as measured by UV/vis spectroscopy (*vide supra*). However, the wavenumber for the ethylenic vibration of the P_3^{520} intermediate is expected at 1533 cm^{-1} according to resonance Raman experiments on the ChR2-C128T variant.[15] The discrepancy in the wavenumber maximum could be due, among other factors, to contributions from amide II vibrations of the opsin in the IR spectra, contributions not present in resonance Raman spectra.

Retinal Fingerprint Vibrations Indicate Biphasic Dark-State Recovery and an All-*trans* Retinal Conformation in P_4^{480}. The five C–C bonds of the retinal polyene skeleton display coupled vibrational modes.[56,57] Several of the resulting vibrational modes show significant Raman and IR intensity, giving rise to the so-called retinal fingerprint region, rich in information regarding retinal conformation.[57] As an example, all-*trans*,15-*anti* retinal of the dark state of light-adapted bR displays three strong IR bands at 1252, 1202, and 1167 cm^{-1} with a smaller one at 1214 cm^{-1}.[42] In contrast, 13-*cis*,15-*syn* retinal in the dark state of light-adapted *Anabaena* sensory

DOI: 10.1021/ja5108595
J. Am. Chem. Soc. 2015, 137, 1850–1861

rhodopsin (ASR) shows only IR bands at 1180 and 1230 cm^{-1}.[61,62] In the light-induced IR difference spectrum of ChR2-WT, three intense negative bands are observed at 1240, 1200, and 1154 cm^{-1}, akin to light-adapted bR and, thus, indicative for all-*trans*,15-*anti* retinal being the predominant retinal isomer of the dark state.[16] We observe similar negative bands at 1237, 1202, and 1152 cm^{-1} in ChR2-E123T (Figures 3 and 8a). The

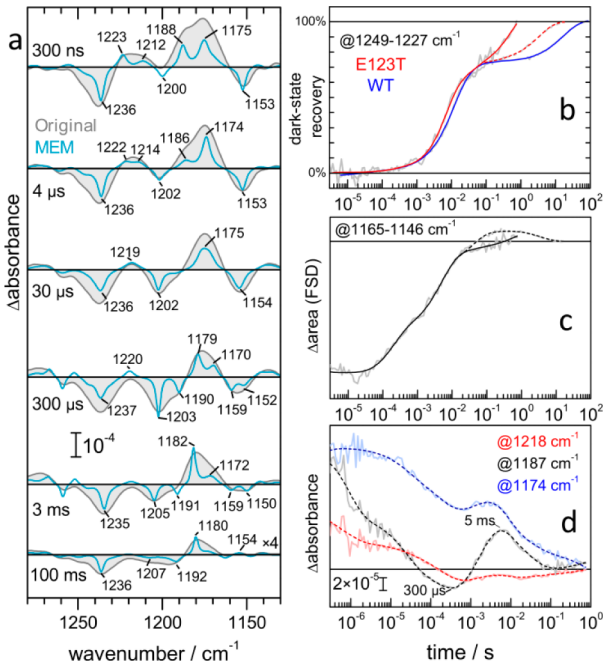

Figure 8. Analysis of the retinal fingerprint region of ChR2-E123T. (a) FT-IR difference spectra of ChR2-E123T at selected times (gray lines), processed by MEM (light blue lines). (b) Experimental and fitted kinetics for the dark-state recovery of the retinal for ChR2-WT (gray and blue traces, respectively) and ChR2-E123T (gray and red traces), obtained from the area between 1249 and 1227 cm^{-1} in the FSD spectra. A 1 Hz (continuous traces) or 0.05 Hz repetition rate (dashed traces) was used for ChR2-E123T. (c) Experimental (gray traces) and fitted (black traces) area between 1165 and 1146 cm^{-1}, integrated in the FSD spectra, reflecting the conversion of retinal from the 13-*cis* to the all-*trans* conformation. Dashed traces correspond to complementary rapid-scan experiments at 0.05 Hz repetition rate. (d) Transient absorption changes at 1187 cm^{-1} (black trace), 1218 cm^{-1} (red trace), and 1174 cm^{-1} (blue trace), for experimental (continuous traces) and fitted (dashed traces) data. See text for the band assignment.

recovery of the area of these three negative bands to zero encodes information about the kinetics of the relaxation of the retinal back to the all-*trans*,15-*anti* dark-state conformation.

In bR, the area of the band at 1252 cm^{-1} (C_{14}–C_{15} + C_{12}–C_{13} coupled with Lys216)[56] was found to be a good reporter to follow the recovery kinetics of the dark state with all-*trans* retinal.[41,63] Using the same approach, we have previously shown that the dark-state recovery is markedly biphasic in ChR2-WT,[16] as reproduced in Figure 8b (blue line). We assigned each phase to a different pathway for dark-state recovery: the principal (75% of the amplitude) directly from the P_3^{520} intermediate and the secondary (25% of the amplitude) from the P_4^{480} intermediate,[16] leading to the proposal of a branched photocycle.[7] To infer the dark-state recovery kinetics in ChR2-E123T, we probed the area of the band at 1237 cm^{-1}. We also observe biphasic dark-state recovery kinetics for the all-*trans* photocycle (Figure 8b, red line). For accurate results on the kinetics of the slow phase of the recovery, we also performed rapid-scan FT-IR experiments with laser excitation only every 20 s (Figure 8b, dashed red line). The decay of the slow recovery phase is around 5 times faster in ChR2-E123T than in ChR2-WT: τ = 3 s versus 16 s for the slower time constant (see Table S1, Supporting Information), in good agreement with results from UV/vis (Figure 3e and Table S1, Supporting Information), and the 10 times faster dark adaptation of the channel in ChR2-E123T measured by electrophysiology.[25]

The area of the negative band at 1167 cm^{-1} in bR, mostly C_{10}–C_{11} + C_{12}–C_{13} stretching,[56] was shown to report on the kinetics of thermal reisomerization of the retinal from the 13-*cis* to all-*trans* conformation,[41] occurring in the transition between the N and O intermediates. We analyzed the time evolution of the homologous band at 1152 cm^{-1} of ChR2-E123T. The area of this band decreases from 100 μs onward, and vanishes ~50 ms after photoexcitation (Figure 8c), a process accompanied by its apparent split into two bands at 1159 and 1150 cm^{-1} (see Figure 8a, blue line). We account for both events by the appearance of an overlapping positive band at ~1154 cm^{-1}. An analogous phenomenon occurs in bR[64] and in hR[52] when the retinal reisomerizes from 13-*cis* back to all-*trans* in the O intermediate. From the above results, we conclude that the P_4^{480} intermediate, the only intermediate present above 50 ms in ChR2-E123T (see Figure 3a), contains all-*trans* retinal, albeit with fingerprint vibrations (and conformation) differing from the all-*trans* retinal of the dark state. This conclusion is supported by previous evidence regarding retinal extraction experiments after illumination.[7]

Regarding retinal fingerprint bands for the 13-*cis* retinal in the dark state, a resonance Raman study on ChR2-WT assigned a band at 1183 cm^{-1} to 13-*cis*,15-*syn* retinal,[19] an assignment derived from previous work on dark-adapted bR.[55] The light-induced IR difference spectrum of ChR2-WT at 80 K displayed a negative band at 1183 cm^{-1},[14,15] assigned to the photoisomerization of dark-state 13-*cis*,15-*syn* retinal.[7] However, we were not able to resolve such a negative band in our time-resolved FT-IR experiments on ChR2-E123T (Figures 3 and 8) or ChR2-WT,[16] possibly due to insufficient spectral resolution.

Retinal Fingerprint Vibrations of the Photoproducts from the All-*trans* and 13-*cis* Photocycles. Positive bands in the retinal fingerprint region are assignable to photoproducts from the photocycles of all-*trans* and 13-*cis* retinal. A broad positive band appears between ~1190 and 1170 cm^{-1}, and a smaller one appears around 1220 cm^{-1} (Figures 3 and 8a). Both of them were previously observed in ChR2-WT.[16] These two broad positive bands contain overlapping components, partially resolved after MEM deconvolution (Figure 8a).

The band at ~1187 cm^{-1} most likely originates from 13-*cis* photoproducts of the all-*trans* photocycle because the frequency is akin to the K, L, and N intermediates of bR and other microbial rhodopsins.[52,53,64−66] A similar band was previously reported in ChR2-WT at 1188 and 1191 cm^{-1} by time-resolved[16] and by cryo-FT-IR spectroscopy,[17,18] respectively. Furthermore, the temporal evolution of the absorption intensity at ~1187 cm^{-1} (Figure 8d) follows a pattern of intensity changes familiar to that of bR at a similar wavenumber.[67,68] The intensity decreases first and increases later due to the coupling between the dipole moment of the C–C stretching modes of the polyene chain with the protonation state of the SB, a useful IR marker to follow

DOI: 10.1021/ja5108595
J. Am. Chem. Soc. 2015, 137, 1850−1861

Table 1. Assignment of Main Vibrational Bands of ChR2-E123T

position[a]	vibration	assignment	state[b]
~1760 (+)	C=O stretch	Asp156	P_{1b}^{500}
~1742 (+)	C=O stretch	Asp156	P_{1a}^{500} + P_2^{390}
1737 (−)	C=O stretch	Asp156	$ChR2^{470}$
1663 (−)	amide I	transmembrane α-helices	$ChR2^{470}$
1655 (−)	C=N stretch	retinal Schiff base	$ChR2^{470}$
1623 (+)	C=N stretch	retinal Schiff base	P_1^{500}
1558 (−)	C=C stretch	13-*cis* retinal	$ChR2^{460}$
1552 (−)	C=C stretch	all-*trans* retinal	$ChR2^{470}$
1541 (+)	C=C stretch	13-*cis* retinal	P_1^{500}
1528 (+)	C=C stretch	all-*trans* retinal	I_2
1514 (+)	C=C stretch	all-*trans* retinal	I_1
1237 (−)	C—C stretch	all-*trans* retinal	$ChR2^{470}$
1220 (+)	C—C stretch	all-*trans* retinal	I_1
1202 (−)	C—C stretch	all-*trans* retinal	$ChR2^{470}$
1188−1182 (+)	C—C stretch	13-*cis* retinal[c]	P_1^{500} + P_3^{520}
~1175 (+)	C—C stretch	all-*trans* retinal	I_1 + I_2 + P_4^{480}
1152 (−)	C—C stretch	all-*trans* retinal	$ChR2^{470}$ + P_4^{480}
988 (+)	HOOP[d]	retinal	P_1^{500}

[a]In cm^{-1}. [b]States of the photocycle of ChR2 are named following the nomenclature in Figure 9. [c]The P_2^{390} state contributes negligibly because of its deprotonated SB. [d]Hydrogen out-of-plane wagging.

protonation changes of the SB.[41,68] In ChR2-E123T, the intensity at 1187 cm^{-1} reaches a minimum at 300 μs (Figure 8d), which agrees well with the maximal accumulation of P_2^{390} in hydrated films (Figure S2, Supporting Information). The intensity at 1187 cm^{-1} recovers following SB reprotonation, reaching a maximum at 5 ms (maximal accumulation of P_3^{520}), and then approaches to zero as the photocycle completes (Figure 8d). The recovery of the intensity after SB reprotonation is concurrent with a 5 cm^{-1} spectral downshift from 1187 to 1182 cm^{-1} (Figure 8a), resembling the spectral shift between the K/L (~1189 cm^{-1}) and the N (~1184 cm^{-1}) intermediates in bR.[64,65]

The most intense positive band in the retinal fingerprint region of ChR2-E123T appears at ~1175 cm^{-1} (Figures 3 and 8a), as in ChR2-WT.[16] A positive band at 1178−1176 cm^{-1} has been reported in various microbial rhodopsins with significant content of 13-*cis* retinal in the dark state (e.g., *Gloeobacter* rhodopsin, *Neurospora* rhodopsin, ASR, and proteorhodopsins), and assigned to all-*trans* intermediates formed during the 13-*cis* photocycle.[66,69−71] It is noted that all-*trans* intermediates formed in the all-*trans* photocycle, such as the P_4^{480} state, could contribute as well with a positive band at a similar wavenumber, although at later times. This may explain why the absorption at 1175 cm^{-1} decays until ~1 ms but then it rises again and persists until the completion of the all-*trans* photocycle (Figure 8a).

Finally, the small positive band at ~1220 cm^{-1} is present only in the nano- and microsecond ranges (Figure 8a and d). A positive band at this wavenumber has not been reported for any microbial rhodopsin to our knowledge. An exception is the T90A mutant of bR,[72] a variant with an unusual large content of 13-*cis* retinal in the light-adapted form.[73] Therefore, we assign the band at 1220 cm^{-1} exclusively to photoproduct(s) of the 13-*cis* photocycle, which vanish in less than 1 ms.

In summary, the evolution of retinal fingerprint bands assignable to photoproducts of the 13-*cis* photocycle is coherent with the decay of the ethylenic mode assigned to the 13-cis retinal in the dark-state of ChR2. Both support the conclusion that the 13-*cis* photocycle is completed 1 ms after photoexcitation.

GENERAL DISCUSSION

We have performed a detailed analysis of the photocycle of the fast-cycling functional ChR2-E123T variant of channelrhodopsin-2, also known as ChETA.[25] We have combined time-resolved UV/vis and IR spectroscopies from the early nanoseconds until the completion of the photocycle. From time-resolved absorption changes of specific vibrational bands, compiled in Table 1, we obtained new insights into the photocycle of the E123T variant of ChR2 and, in extension, into the functional mechanism of channelrhodopsins.

Pre-Gating Conformational Changes. There is a hierarchy of structural changes occurring in ChR2 prior to when the conductive state is formed, i.e., before ~200 μs, to which we refer here as pre-gating conformational changes. Time-resolved IR studies have explored the picosecond and micro-millisecond time ranges of the photocycle of ChR2,[16,17,74] leaving conformational changes that might occur in the nanosecond range unresolved. As noted before,[14,15,17] notable spectral changes proceed concurrently with retinal photoisomerization, remarkably large when compared to other microbial and animal rhodopsins.[7] Particularly, an intense negative band in the amide I region at ~1663 cm^{-1} (Figure 3) is formed in the sub-picosecond time range.[17] Here, we have further confirmed using the E123T variant that the band at ~1663 cm^{-1} does not arise from the C=N stretching vibration of the SB, clearly resolved at 1655 cm^{-1} (Figure 5a), in agreement with previous resonance Raman experiments.[19] The frequency of the band at ~1663 cm^{-1} is resistant to H/D exchange (Figure 5a) excluding significant contributions of amino acid side chain vibrations. Most reasonable, the band at ~1663 cm^{-1} originates from an amide I vibration delocalized along a transmembrane helix. We propose that a light-induced structural distortion, likely due to the steric clash with the isomerizing retinal, might locally distort a previously regular transmembrane helix and, thus, reduce the delocalization and extinction coefficient of the amide I vibration. Incidentally, we

DOI: 10.1021/ja5108595
J. Am. Chem. Soc. 2015, 137, 1850−1861

assigned the C=N vibration of the SB after isomerization at 1623 cm^{-1} (Figure 5a), suggesting that the hydrogen bond of the SB gets drastically weakened after retinal photoisomerization, albeit not fully broken.

We observed spectral changes rising with a half-time of ~200 ns in ChR2-E123T (Figure 4), which are resolved here for the first time in any channelrhodopsin. These pre-gating conformational changes affect bands in the amide I and C=O stretching regions of the (protonated) carboxylic group of D156. Similar spectral changes occurring in the same time range are also observed in ChR2-WT (Figure S9, Supporting Information). The spectral changes in amide I bands are of more ambiguous interpretation, but the upshift of the C=O stretch frequency from 1742 to 1760 cm^{-1} suggests a transient weakening of the interhelical H-bond between D156 and C128 (the DC gate as these two residues connect helices D and C).[36] This weakening might originate from the relative movement or rotation of helices D and C at around 200 ns after retinal photoisomerization. These newly resolved spectral changes partially reconcile notable dissimilarities between the IR difference spectrum of the P_1^{500} intermediate measured by cryo-FT-IR[15] and time-resolved FT-IR spectroscopy with microsecond resolution.[16] It also confirms the presence of two P_1^{500} substates, with a $t_{1/2}$ value for their transition of 200 ns in ChR2-E123T (Figure 4b) and of 400 ns in ChR2-WT (Figure S9, Supporting Information). These two intermediates are hardly distinguishable by UV/vis spectroscopy and, thus, contain a similar retinal conformation and electrostatic environment. The final pre-gating changes relate to the deprotonation of the SB and have been discussed elsewhere.[7,16]

Incidentally, while the transition between the two P_1^{500} intermediates is similarly fast in ChR2-E123T and ChR2-WT ($t_{1/2}$ ≈ 200 ns vs 400 ns), the decay of the late P_1^{500} intermediate is almost 10 times faster in ChR2-E123T than in ChR2-WT ($t_{1/2}$ ≈ 40 μs vs 300 μs), as concluded from the kinetics of absorbance changes at 1760 cm^{-1} (compare Figure 4b and Figure S9b, Supporting Information). This kinetic alteration in the E123T variant might explain why the band at 1760 cm^{-1} was recently misassigned to E123.[18]

How pre-gating structural and protonation changes are linked to the opening of the channel and the onset of cation permeation remains elusive in full atomistic detail, and will require further studies. However, the distortion of helices by retinal isomerization, followed by changes in interhelical interactions and continued by changes in H-bonding networks induced by protonation changes, are likely key elements for the coupling between retinal isomerization and the conformational changes required to form the conductive state.

Photocycles from All-*trans* and 13-*cis* Retinal. ChR2 contains a mixture of all-*trans* (~70%) and 13-*cis* (~30%) retinal isomers in the dark-state form.[19] The isomeric ratio is not influenced by the E123T exchange.[24] The photocycle of any of these two forms could, in principle, be functional. In ChR2-E123T, we were able to resolve retinal ethylenic bands specific for the dark-state form of all-*trans* and 13-*cis* retinal at 1552 and 1558 cm^{-1} with the assistance of a band-narrowing method. Thus, we conclude that both retinal isomers contribute to the photoreaction for light-adapted samples (Figure 7a). For ChR2-WT, the separation of the ethylenic bands of all-*trans* and 13-*cis* retinal was not successful, but their presence was suggested by the asymmetry of a band at 1553 cm^{-1} (Figure S4, Supporting Information). From the time evolution of the area of the 1558 cm^{-1} band, we concluded that the recovery of the 13-*cis* photocycle of ChR2-E123T occurs with a half-time slightly faster than 1 ms (Figure 7a).

The photocycle of 13-*cis* retinal involves at least two intermediates, presumably containing all-*trans* retinal (Figure 9b). The recovery of the 13-*cis* photocycle is faster than most of

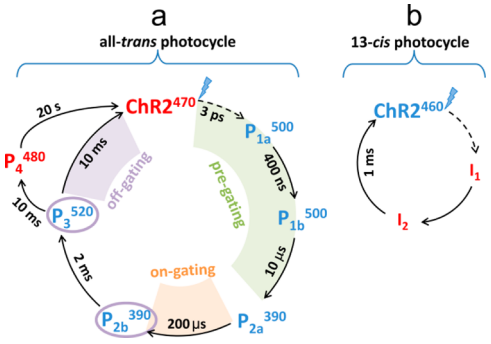

Figure 9. Proposed photocycles of ChR2. (a) Photocycle starting from the photoisomerization of all-*trans* retinal. (b) Photocycle initiated by excitation of 13-*cis* retinal. Light-induced reactions are indicated by dashed arrows, and thermally activated reactions, by continuous arrows. Intermediates containing all-*trans* and 13-*cis* retinal are colored in red and blue, respectively. Conductive intermediates are enclosed in a circle. The time constants are approximate and refer to ChR2-WT, except for the recovery of $ChR2^{460}$ (1 ms), taken from ChR2-E123T.

the proton transfer reactions,[16] supporting that only the all-*trans* photocycle is linked to the proton-pumping activity of ChR2, as was also concluded for bR before.[75,76]

The fact that the ethylenic bands of all-*trans* and 13-*cis* retinal of dark-state ChR2 could be only resolved by mathematical band-narrowing may add ambiguity to some of our conclusions, especially regarding the time for completion of the 13-*cis* photocycle. As additional support, the analysis of the retinal photoproducts in the ethylenic and fingerprint regions (Figures 7e and 8a), relying much less on band-narrowing methods, is coherent with the view that the 13-*cis* photocycle is completed in ~1 ms. Still, the spectral resolution and kinetic characterization of the all-*trans* and 13-*cis* photocycles should be further attempted using alternative approaches, to confirm and extend our results. The use of isotopically labeled retinal might allow for the resolution of ethylenic bands from all-*trans* and 13-*cis* retinal without the need of band-narrowing techniques. For instance, the use of 13-^{13}C retinal incremented the spectral separation of the main ethylenic band of 13-*cis* and all-*trans* retinal from 9 to 16 cm^{-1} in bR,[54,55] and could have a similar effect in ChR2.

It has been shown that two parallel photocycles are required to quantitatively reproduce the photocurrents of ChR2 under photostationary conditions.[21,22,77,78] Two open (conductive) states, O1 and O2, are reached by photoexcitation of two closed (parent) states, C1 and C2.[21,22,77,78] The conductive state O2 exhibits slower off-gating kinetics than O1 ($t_{1/2}$ ≈ 40 ms for O2 vs $t_{1/2}$ ≈ 10 ms for O1 in wild type ChR2), and the C2 state relaxes thermally to the C1 state with $t_{1/2}$ ≈ 10 s.[22,78] The photocycle starting from the parent state C1 is expected to be equivalent to that observed in most time-resolved spectroscopic studies, performed by excitation with short (10 ns) light pulses;[16,17,60,74] i.e., the C1 state is equivalent to the dark-state $ChR2^{470}$ (Figure 9a). This is supported by the very similar decay of the O1 state and the P_3^{520} intermediate in wild type ChR2 and in the D156E and D253E variants.[16] It was

DOI: 10.1021/ja5108595
J. Am. Chem. Soc. 2015, 137, 1850−1861

recently suggested that the O2 state could originate from the photocycle of 13-*cis* retinal.[24] Among other problems, detailed elsewhere,[7] this suggestion directly conflicts with our current finding that the 13-*cis* retinal photocycle is completed in around 1 ms (Figure 9b), way ahead of the 40 ms inferred for the decay of the O2 state.

CONCLUDING REMARKS

We have confirmed that the E123T variant of ChR2 shows a native-like photocycle with some minor kinetic and spectral differences with respect to the WT form, namely, an ∼5 times faster decay of the P_4^{480} intermediate to the initial dark state. The red-shift in the retinal absorption of ChR2-E123T with respect to ChR2-WT suggests that E123 remains ionic across the entire photocycle.

We have presented, for the first time, evidence for conformational changes in a channelrhodopsin taking place in the nanosecond range. The corresponding spectral changes are silent to UV/vis spectroscopy but lead to spectral changes in the amide I and carboxylic C═O regions. These structural changes of the apoprotein rise with a half-life of 200 ns in ChR2-E123T and of 400 ns in ChR2-WT, and presumably form part of a hierarchy of conformational changes connecting retinal photoisomerization to the onset of cation permeation. Because P_1^{500} is the only intermediate present in the nanosecond range, we conclude the existence of two P_1^{500} substates in ChR2 with similar retinal conformation and electrostatic environment but differing in the structure of the apoprotein.

ChR2 contains in the dark state a mixture of all-*trans* and 13-*cis* retinal. The contribution of 13-*cis* retinal to cation permeation is disputed. It has been shown that quantitatively reproducing the photocurrents of ChR2 under continuous illumination requires two parallel photocycles with open states decaying with time constants of 10 and 40 ms. Here, we resolved the photocycles from all-*trans* and 13-*cis* retinal from the analysis of the retinal C═C and C—C stretchings, sensitive to the retinal conformation. While most of the all-*trans* photocycle ends with a $t_{1/2}$ value of 10 ms, our results indicate that the 13-*cis* photocycle ends in about 1 ms, much too early to be the second photocycle contributing to cation permeation. Therefore, it is evident that the formation of a conductive state in ChR2 is limited to photoproducts of the all-*trans* photocycle.

EXPERIMENTAL SECTION

Sample Preparation. For spectroscopic studies, a truncated construct (amino acids 1−315) of ChR2-E123T with an added His-tag was heterologously expressed in *Pichia pastoris* and purified by NTA affinity chromatography. The purified protein was solubilized in 0.2% decyl maltoside, 100 mM NaCl, and 20 mM Hepes (pH 7.4). For flash photolysis, ChR2-E123T was diluted in the same buffer to give a final absorption of 0.4 in a cuvette of 1 cm path length. For FT-IR and QCL experiments, ChR2-E123T was concentrated to ∼15 mg/mL, and ∼2 μL was spread and gently dried on top of a BaF_2 window. The film was rehydrated from the vapor phase of a glycerol/H_2O mixture (3:7 wt/wt) and tightly closed with a second window using a silicone spacer of 1 mm thickness. The molar ratio of water, detergent, and protein was determined from the IR absorption spectra to be ∼3000:75:1 after equilibration for ∼1 h (Figure S5, Supporting Information), as described.[79] For experiments in D_2O, the film was rehydrated using a per-deuterated glycerol/D_2O mixture (3:7 wt/wt). The remaining amount of H_2O present was about 5%, as determined from the IR absorption spectrum (Figure S6, Supporting Information).

Photoexcitation. We used an optical parametric oscillator (OPTA) driven by the third harmonic of a Nd:YAG laser (Quanta-Ray; Spectra-Physics). The sample was excited by a short (∼10 ns) laser pulse of λ = 470 nm (440 nm for ChR2-WT) with 3 mJ/cm^2 energy density at the sample, leading to the photoconversion of ∼10% of the molecules.

Time-Resolved FT-IR Spectroscopy. Time-resolved FT-IR experiments were performed at 8 cm^{-1} spectral resolution, using a commercial FT-IR spectrometer (Vertex 80v; Bruker) equipped with a photovoltaic MCT detector. The sample holder was kept at 25 °C using a circulating water bath (F25; JULABO). We performed time-resolved rapid-scan FT-IR experiments at a 240 kHz mirror speed, tracing kinetics from ∼20 ms onward. Experiments at a fast (1 Hz) and a slow (0.05 Hz) repetition rate gave similar spectra (Figure S7, Supporting Information), supporting the use of a 1 Hz repetition rate in the step-scan FT-IR experiments. For time-resolved step-scan FT-IR experiments, we performed both DC-coupled and AC-coupled experiments to cover the time range from nanoseconds to several hundreds of milliseconds. The DC output of the preamplifier was alternatively digitized at a 160 and 25 kHz sampling rate, covering a time range from −12.5 to 125 ms and from −80 to 800 ms, respectively. The AC output of a fast preamplifier was digitized at a 100 MHz sampling rate, from −20 to 200 μs. For the AC-coupled experiments, we retrieved the phase from a DC interferogram and signal changes were converted into absorption changes using an appropriately scaled DC interferogram. Time traces were logarithmically averaged to ∼20 points/decade (see the Supporting Information for further technical details).

Time-Resolved Tunable Quantum Cascade Laser (QCL) Spectroscopy. We developed a spectrometer using a tunable external cavity quantum cascade laser as the IR source (Daylight Solutions), which will be described in more detail elsewhere. Briefly, the setup is typical for a flash-photolysis experiment in transmission configuration. The tunable monochromatic IR beam from a QCL was directed after attenuation to the sample. The transmitted light was focused to a photovoltaic MCT detector connected to a fast preamplifier. The spectrometer was purged with dry air, and the temperature of the sample holder was ∼23 °C during the experiments. The DC signal from the preamplifier was digitized by an oscilloscope at 250 MHz (from −1 μs until 40 ms after photoexcitation), or by two oscilloscopes (for measurements extending up to 500 ms). The signal changes were converted into absorption changes using 500 pretrigger points, and logarithmically averaged to 50 points/decade. This process was repeated from 1610 to 1680 cm^{-1} in 1 cm^{-1} steps and from 1700 to 1780 cm^{-1} in 0.5 cm^{-1} steps at a laser excitation rate of 0.33 Hz. For experiments in D_2O, the repetition rate was reduced to 0.2 Hz. The resulting spectra were convoluted in the Fourier domain by using a Gaussian to obtain spectra at formally 4 cm^{-1} resolution.

Static and Time-Resolved UV/vis Experiments. UV/vis absorption spectra were measured with a commercial spectrometer (UV-2450 PC; Shimadzu). Transient absorption changes in the UV/vis were measured in a commercial flash photolysis instrument (LKS80; Applied Photophysics). The cuvette holder was kept at 25 °C using a circulating water bath (F25; JULABO). The transients were recorded on two time scales. For the faster time range (∼100 ns to 200 μs), we used the Xe arc lamp in pulse mode and the data was sampled at a rate of 1 GHz. For the slower range (∼10 μs to 10 s), the lamp worked in continuous mode and the data was sampled at 100 kHz. The laser repetition rate was in both cases 0.08 Hz. The process was repeated from 300 to 700 nm in 20 nm steps. The fast and slow channels were logarithmically averaged to 100 points per decade. For display purposes, the data was spline-interpolated to 1 nm using the Matlab "interp1" built-in function. Similar experiments were performed also on a hydrated film of ChR2-E123T deposited in a BaF_2 window, and transient absorption changes were measured at 380, 480, and 540 nm.

Data Analysis. Time-resolved step-scan FT-IR, rapid-scan FT-IR, and UV/vis data were subjected to singular value decomposition (SVD) for noise filtering, as implemented in the "svd" function of Matlab with some modifications,[80] and reconstructed with seven, two,

DOI: 10.1021/ja5108595
J. Am. Chem. Soc. 2015, 137, 1850−1861

and seven SVD components, respectively. The QCL data was subjected to SVD only in the 1780−1700 cm^{-1} region, retaining seven SVD components. Global exponential fitting was performed in combination with SVD (see time constants in Table S1, Supporting Information). We used several exponentials plus an offset when fitting time-resolved UV/vis and rapid-scan FT-IR data. A similar model was used to fit the time-resolved step-scan FT-IR and QCL data but taking into account the response function of the detector/preamplifier system, modeled as a Gaussian (see Figure S8, Supporting Information). The number of exponentials and initial values for the time constants used in the fitting was guided by a lifetime distribution analysis. Lifetime distributions were estimated using the maximum entropy method, with the regularization value automatically determined using the L-curve method.[81] Spectral band narrowing was performed by Fourier self-deconvolution (FSD)[40] and by deconvolution by the maximum entropy method (MEM).[38] FSD was performed using a Lorentzian width of 12 cm^{-1}, a narrowing factor of 1.5, and a Bessel filter as described elsewhere.[41] MEM was performed using a Lorentzian width of 8 cm^{-1}, taking into account the instrumental spectral resolution and apodization function.

■ ASSOCIATED CONTENT

Supporting Information

Supplementary experimental section, supplementary table, and supplementary figures. Table S1 - Time constants from global exponential fitting of time-resolved UV/vis and IR data. Figure S1 - Kinetics of ChR2-E123T in a hydrated film versus solution at 380 and 540 nm. Figure S2 - Kinetics at 1737 cm^{-1} from step-scan FT-IR spectroscopy. Figure S3 - Comparison of the kinetics at 1541 cm^{-1} for ChR2-E123T and ChR2-WT. Figure S4 - FT-IR difference spectrum at 6 μs of the ethylenic bands of ChR2-WT and ChR-E123T after MEM deconvolution. Figure S5 - FT-IR absorption spectrum of a hydrated film of ChR2-E123T, used to estimate the molar ratio of protein/detergent/water. Figure S6 - FT-IR absorption spectrum of a hydrated film of ChR2-E123T in H_2O and D_2O. Figure S7 - FT-IR difference spectrum 210 ms after photoexcitation, at 1 and 0.05 Hz laser repetition rates. Figure S8 - Example of the fitting of kinetic traces, showing the response time of the detector. Figure S9 - Transient absorption changes of ChR2-WT at 1760, 1737, 1661, and 1634 cm^{-1}. Figure S10 - Spectral comparison of the late P_1^{500} intermediate of ChR2-WT and ChR2-E123T in the carboxylic region. This material is available free of charge via the Internet at http://pubs.acs.org.

■ AUTHOR INFORMATION

Corresponding Author

*victor.lorenz@fu-berlin.de

Notes

The authors declare no competing financial interest.

■ ACKNOWLEDGMENTS

Financial support came from the Deutsche Forschungsgemeinschaft (SFB 1078/B3 to J.H. and B4 to R.S.) and by the Focus Area Nanoscale of the FU Berlin (to J.H.).

■ REFERENCES

(1) Nagel, G.; Ollig, D.; Fuhrmann, M.; Kateriya, S.; Musti, A. M.; Bamberg, E.; Hegemann, P. *Science* **2002**, *296*, 2395.

(2) Nagel, G.; Szellas, T.; Huhn, W.; Kateriya, S.; Adeishvili, N.; Berthold, P.; Ollig, D.; Hegemann, P.; Bamberg, E. *Proc. Natl. Acad. Sci. U. S. A.* **2003**, *100*, 13940.

(3) Bamann, C.; Nagel, G.; Bamberg, E. *Curr. Opin. Neurobiol.* **2010**, *20*, 610.

(4) Zhang, F.; Vierock, J.; Yizhar, O.; Fenno, L. E.; Tsunoda, S.; Kianianmomeni, A.; Prigge, M.; Berndt, A.; Cushman, J.; Polle, J.; Magnuson, J.; Hegemann, P.; Deisseroth, K. *Cell* **2011**, *147*, 1446.

(5) Stehfest, K.; Hegemann, P. *ChemPhysChem* **2010**, *11*, 1120.

(6) Mattis, J.; Tye, K. M.; Ferenczi, E. A.; Ramakrishnan, C.; O'Shea, D. J.; Prakash, R.; Gunaydin, L. A.; Hyun, M.; Fenno, L. E.; Gradinaru, V.; Yizhar, O.; Deisseroth, K. *Nat. Methods* **2012**, *9*, 159.

(7) Lórenz-Fonfría, V. A.; Heberle, J. *Biochim. Biophys. Acta* **2014**, *1837*, 626.

(8) Lin, J. Y. *Exp. Physiol.* **2010**, *96*, 19.

(9) Spudich, J. L.; Yang, C. S.; Jung, K. H.; Spudich, E. N. *Annu. Rev. Cell. Dev. Biol.* **2000**, *16*, 365.

(10) Ernst, O. P.; Lodowski, D. T.; Elstner, M.; Hegemann, P.; Brown, L. S.; Kandori, H. *Chem. Rev.* **2014**, *114*, 126.

(11) Kato, H. E.; Zhang, F.; Yizhar, O.; Ramakrishnan, C.; Nishizawa, T.; Hirata, K.; Ito, J.; Aita, Y.; Tsukazaki, T.; Hayashi, S.; Hegemann, P.; Maturana, A. D.; Ishitani, R.; Deisseroth, K.; Nureki, O. *Nature* **2012**, *482*, 369.

(12) Krause, N.; Engelhard, C.; Heberle, J.; Schlesinger, R.; Bittl, R. *FEBS Lett.* **2013**, *587*, 3309.

(13) Sattig, T.; Rickert, C.; Bamberg, E.; Steinhoff, H. J.; Bamann, C. *Angew. Chem., Int. Ed. Engl.* **2013**, *52*, 9705.

(14) Ritter, E.; Stehfest, K.; Berndt, A.; Hegemann, P.; Bartl, F. J. *J. Biol. Chem.* **2008**, *283*, 35033.

(15) Radu, I.; Bamann, C.; Nack, M.; Nagel, G.; Bamberg, E.; Heberle, J. *J. Am. Chem. Soc.* **2009**, *131*, 7313.

(16) Lórenz-Fonfría, V. A.; Resler, T.; Krause, N.; Nack, M.; Gossing, M.; Fischer von Mollard, G.; Bamann, C.; Bamberg, E.; Schlesinger, R.; Heberle, J. *Proc. Natl. Acad. Sci. U. S. A.* **2013**, *110*, E1273.

(17) Neumann-Verhoefen, M. K.; Neumann, K.; Bamann, C.; Radu, I.; Heberle, J.; Bamberg, E.; Wachtveitl, J. L. *J. Am. Chem. Soc.* **2013**, *35*, 6968.

(18) Kuhne, J.; Eisenhauer, K.; Ritter, E.; Hegemann, P.; Gerwert, K.; Bartl, F. *Angew. Chem., Int. Ed. Engl.* **2015**, in press.

(19) Nack, M.; Radu, I.; Bamann, C.; Bamberg, E.; Heberle, J. *FEBS Lett.* **2009**, *583*, 3676.

(20) Muders, V.; Kerruth, S.; Lórenz-Fonfría, V. A.; Bamann, C.; Heberle, J.; Schlesinger, R. *FEBS Lett.* **2014**, *588*, 2301.

(21) Hegemann, P.; Ehlenbeck, S.; Gradmann, D. *Biophys. J.* **2005**, *89*, 3911.

(22) Nikolic, K.; Grossman, N.; Grubb, M. S.; Burrone, J.; Toumazou, C.; Degenaar, P. *Photochem. Photobiol.* **2009**, *85*, 400.

(23) Schneider, F.; Gradmann, D.; Hegemann, P. *Biophys. J.* **2013**, *105*, 91.

(24) Ritter, E.; Piwowarski, P.; Hegemann, P.; Bartl, F. J. *J. Biol. Chem.* **2013**, *288*, 10451.

(25) Gunaydin, L. A.; Yizhar, O.; Berndt, A.; Sohal, V. S.; Deisseroth, K.; Hegemann, P. *Nat. Neurosci.* **2010**, *13*, 387.

(26) Scholz, F.; Bamberg, E.; Bamann, C.; Wachtveitl, J. *Biophys. J.* **2012**, *102*, 2649.

(27) Wanko, M.; Hoffmann, M.; Frauenheim, T.; Elstner, M. *J. Comput.-Aided Mol. Des.* **2006**, *20*, 511.

(28) Altun, A.; Yokoyama, S.; Morokuma, K. *Photochem. Photobiol.* **2008**, *84*, 845.

(29) Takahashi, T.; Yan, B.; Mazur, P.; Derguini, F.; Nakanishi, K.; Spudich, J. L. *Biochemistry* **1990**, *29*, 8467.

(30) Watanabe, H. C.; Welke, K.; Sindhikara, D. J.; Hegemann, P.; Elstner, M. *J. Mol. Biol.* **2013**, *425*, 1795.

(31) Tittor, J.; Haupts, U.; Haupts, C.; Oesterhelt, D.; Becker, A.; Bamberg, E. *J. Mol. Biol.* **1997**, *271*, 405.

(32) Chung, H. S.; Tokmakoff, A. *J. Phys. Chem. B* **2006**, *110*, 2888.

(33) Zhang, X.; Chien, E. Y.; Chalmers, M. J.; Pascal, B. D.; Gatchalian, J.; Stevens, R. C.; Griffin, P. R. *Anal. Chem.* **2010**, *82*, 1100.

(34) Grechko, M.; Zanni, M. T. *J. Chem. Phys.* **2012**, *137*, 184202.

(35) Bamann, C.; Gueta, R.; Kleinlogel, S.; Nagel, G.; Bamberg, E. *Biochemistry* **2010**, *49*, 267.

(36) Nack, M.; Radu, I.; Gossing, M.; Bamann, C.; Bamberg, E.; von Mollard, G. F.; Heberle, J. *Photochem. Photobiol. Sci.* **2010**, *9*, 194.

(37) Stephenson, D. S. *Prog. NMR Spectrosc.* **1988**, *20*, 515.

DOI: 10.1021/ja5108595
J. Am. Chem. Soc. 2015, 137, 1850−1861

(38) Lórenz-Fonfría, V. A.; Padrós, E. *Appl. Spectrosc.* **2005**, *59*, 474.
(39) Goormaghtigh, E.; Cabiaux, V.; Ruysschaert, J. M. *Subcell. Biochem.* **1994**, *23*, 363.
(40) Kauppinen, J. K.; Moffatt, D. J.; Mantsch, H. H.; Cameron, D. G. *Appl. Spectrosc.* **1981**, *35*, 271.
(41) Lórenz-Fonfría, V. A.; Kandori, H.; Padrós, E. *J. Phys. Chem. B* **2011**, *115*, 7972.
(42) Maeda, A. *Isr. J. Chem.* **1995**, *35*, 387.
(43) Gerwert, K.; Siebert, F. *EMBO J.* **1986**, *5*, 805.
(44) Ito, S.; Kato, H. E.; Taniguchi, R.; Iwata, T.; Nureki, O.; Kandori, H. *J. Am. Chem. Soc.* **2014**, *136*, 3475.
(45) Nakamichi, H.; Oka, T. *Angew. Chem., Int. Ed.* **2006**, *45*, 1.
(46) Eyring, G.; Mathies, R. *Proc. Natl. Acad. Sci. U. S. A.* **1979**, *76*, 33.
(47) Hayashi, S.; Tajkhorshid, E.; Kandori, H.; Schulten, K. *J. Am. Chem. Soc.* **2004**, *126*, 10516.
(48) Lanyi, J. K. *Mol. Membr. Biol.* **2004**, *21*, 143.
(49) Rödig, C.; Chizhov, I.; Weidlich, O.; Siebert, F. *Biophys. J.* **1999**, *76*, 2687.
(50) Dioumaev, A. K.; Braiman, M. S. *J. Phys. Chem. B* **1997**, *101*, 1655.
(51) Dioumaev, A. K.; Braiman, M. S. *Photochem. Photobiol.* **1997**, *66*, 755.
(52) Hackmann, C.; Guijarro, J.; Chizhov, I.; Engelhard, M.; Rödig, C.; Siebert, F. *Biophys. J.* **2001**, *81*, 394.
(53) Hein, M.; Wegener, A. A.; Engelhard, M.; Siebert, F. *Biophys. J.* **2003**, *84*, 1208.
(54) Smith, S. O.; Braiman, M. S.; Myers, A. B.; Pardoen, J. A.; Courtin, J. M. L.; Winkel, C.; Lugtenburg, J.; Mathies, R. A. *J. Am. Chem. Soc.* **1987**, *109*, 3108.
(55) Smith, S. O.; Pardoen, J. A.; Lugtenburg, J.; Mathies, R. A. *J. Am. Chem. Soc.* **1987**, *91*, 804.
(56) Babitzki, G.; Mathias, G.; Tavan, P. *J. Phys. Chem. B* **2009**, *113*, 10496.
(57) Smith, S. O.; Lugtenburg, J.; Mathies, R. A. *J. Membr. Biol.* **1985**, *85*, 95.
(58) Althaus, T.; Eisfield, W.; Lohrmann, R.; Stockburger, M. *Isr. J. Chem.* **1995**, *35*, 227.
(59) Aton, B.; Doukas, A. G.; Callender, R. H.; Becher, B.; Ebrey, T. G. *Biochemistry* **1977**, *16*, 2995.
(60) Verhoefen, M. K.; Bamann, C.; Blocher, R.; Förster, U.; Bamberg, E.; Wachtveitl, J. *ChemPhysChem* **2010**, *11*, 3113.
(61) Bergo, V. B.; Ntefidou, M.; Trivedi, V. D.; Amsden, J. J.; Kralj, J. M.; Rothschild, K. J.; Spudich, J. L. *J. Biol. Chem.* **2006**, *281*, 15208.
(62) Kawanabe, A.; Furutani, Y.; Jung, K. H.; Kandori, H. *Biochemistry* **2006**, *45*, 4362.
(63) Lórenz-Fonfría, V. A.; Furutani, Y.; Kandori, H. *Biochemistry* **2008**, *47*, 4071.
(64) Zscherp, C.; Heberle, J. *J. Phys. Chem. B* **1997**, *101*, 10542.
(65) Heßling, B.; Souvignier, G.; Gerwert, K. *Biophys. J.* **1993**, *65*, 1929.
(66) Friedrich, T.; Geibel, S.; Kalmbach, R.; Chizhov, I.; Ataka, K.; Heberle, J.; Engelhard, M.; Bamberg, E. *J. Mol. Biol.* **2002**, *321*, 821.
(67) Freier, E.; Wolf, S.; Gerwert, K. *Proc. Natl. Acad. Sci. U. S. A.* **2011**, *108*, 11435.
(68) Rammelsberg, R.; Huhn, G.; Lübben, M.; Gerwert, K. *Biochemistry* **1998**, *37*, 5001.
(69) Miranda, M. R.; Choi, A. R.; Shi, L.; Bezerra, A. G., Jr.; Jung, K. H.; Brown, L. S. *Biophys. J.* **2009**, *96*, 1471.
(70) Bergo, V.; Spudich, E. N.; Spudich, J. L.; Rothschild, K. J. *Photochem. Photobiol.* **2002**, *76*, 341.
(71) Shi, L.; Yoon, S. R.; Bezerra, A. G., Jr.; Jung, K. H.; Brown, L. S. *J. Mol. Biol.* **2006**, *358*, 686.
(72) Perálvarez-Marín, A.; Márquez, M.; Bourdelande, J. L.; Querol, E.; Padrós, E. *J. Biol. Chem.* **2004**, *279*, 16403.
(73) Simon-Vazquez, R.; Dominguez, M.; Lorenz-Fonfria, V. A.; Alvarez, S.; Bourdelande, J. L.; de Lera, A. R.; Padros, E.; Peralvarez-Marin, A. *PLoS One* **2012**, *7*, e42447.
(74) Eisenhauer, K.; Kuhne, J.; Ritter, E.; Berndt, A. E.; Wolf, S.; Freier, E.; Bartl, F.; Hegemann, P.; Gerwert, K. *J. Biol. Chem.* **2012**, *287*, 6904.
(75) Hofrichter, J.; Henry, E. R.; Lozier, R. H. *Biophys. J.* **1989**, *56*, 693.
(76) Gergely, C.; Ganea, C.; Váró, G. *Biophys. J.* **1994**, *67*, 855.
(77) Stefanescu, R. A.; Shivakeshavan, R. G.; Khargonekar, P. P.; Talathi, S. S. *Bull. Math. Biol.* **2013**, *75*, 2208.
(78) Williams, J. C.; Xu, J.; Lu, Z.; Klimas, A.; Chen, X.; Ambrosi, C. M.; Cohen, I. S.; Entcheva, E. *PLoS Comput. Biol.* **2013**, *9*, e1003220.
(79) Lórenz-Fonfría, V. A.; Heberle, J. *J. Visualized Exp.* **2014**, *88*, e51622.
(80) Lórenz-Fonfría, V. A.; Kandori, H. *J. Am. Chem. Soc.* **2009**, *131*, 5891.
(81) Lórenz-Fonfría, V. A.; Kandori, H. *Appl. Spectrosc.* **2007**, *61*, 428.

DOI: 10.1021/ja5108595
J. Am. Chem. Soc. 2015, 137, 1850−1861